# A MAP IIR FILTER FOR 3D ULTRASOUND

*João Sanches and Jorge S. Marques*

Instituto Superior Técnico / Instituto de Sistemas e Robótica
Av. Rovisco Pais, 1049-001 Lisbon, Portugal

**ABSTRACT**

Bayesian reconstruction methods are slow and have been avoided in 3D ultrasound, since fast algorithms are required. This paper tries to overcome this difficulty by presenting a fast reconstruction algorithm designed in a Bayesian framework, based on data dependent IIR filtering. This allows to obtain the benefits of Bayesian volume reconstruction and the computationally efficiency of IIR recursive filtering. The proposed filter has space varying coefficients which depend on the observed data in each region. The proposed method is evaluated using synthetic and real data. The results are compared with the MAP estimates obtained using a nonlinear optimization method. The proposed IIR recursive filtering algorithm achieves comparable results with the MAP algorithm and is twenty five times faster.

## 1. INTRODUCTION

Free-hand 3D ultrasound aims to reconstruct volumes from a sequence of 2D ultrasound images. A spatial locator sensor is coupled to the ultrasound probe in order to measure the probe position at each instant of time. Several papers have addressed this problem [1]. In most cases, the reconstruction time is a major design constraint. This constraint is imposed by the physicians who want to visualize the results as soon as possible as it happens in 2D ultrasound. This is the reason why most algorithms used in 3D ultrasound are designed in a ad hoc basis aiming to be as simple and fast as possible. For this reason Bayesian methods have been avoid, since they are computationally demanding and time consuming. Bayesian approach has been used with great success on other medical imaging modalities [2] which do not require real time processing, e.g., CT, MRI, SPECT and PET.

This paper[1] tries to overcome this difficulty by presenting a fast reconstruction algorithm design in a Bayesian framework, based on data dependent IIR filtering. This allows to obtain the benefits of Bayesian volume reconstruction and the computational efficiency of the IIR recursive filtering. The proposed filter has space varying coefficients which depend on the observed data in each region.

[1]This work was partially supported by FCT (Heart 3D project).

The algorithm performs reconstructions in two steps. In the first step, a maximum likelihood estimate is computed, based on the available data. In a second step the ML estimation is filtered, using an appropriate IIR filter with space varying parameters, depending on the data.

The performance of the proposed algorithm (IIRMAP) is assessed using synthetic and real data. In each experiment the output of the proposed algorithm is compared with the MAP estimate obtained using nonlinear optimization technique (NLMAP) and the fast algorithm (LMAP) recently proposed in [3]. The reconstruction results are similar and it is shown that the method proposed in this paper is significantly faster than the others two methods.

## 2. MAP RECONSTRUCTION

This section briefly describes the NLMAP reconstruction algorithm. Additional details can be found in [4].

Let $f(x)$ be a function to be estimated, defined in $\Omega \in R^3$, belonging to finite dimension vector space, $F$ with known basis functions, $\phi_i : \Omega \rightarrow R^3$). Therefore $f$ can be expressed as a linear combination of the basis functions,

$$f(x) = \Phi(x)^T U \tag{1}$$

where $\Phi(x) = [\phi_1(x), \phi_2(x), ..., \phi_N(x)]T$ is a vector of basis functions and $U = [u_1, u_2, ..., u_N]$ is a $N \times 1$ vector of coefficients. $\phi_p(x)$ are interpolation functions centered at $\mu_p$, where $p = (i, j, k)$ and $\mu_p$ are the 3D nodes of a cubic 3D grid, $\{0, ..., N-1\}^3$. The coefficients $u_p$ are a discrete 3D signal defined in $R^3 \cap \Omega$.

Let $V = \{x_i, y_i\}$ be the set of observed data: $y_i$ being a noisy observation of $f(x_i)$ and $x_i \in \Omega$. In the case of ultrasound images it is often assumed that the observations $y_i$ (pixel intensities) are independent and identically distributed random variables with Rayleigh distribution [5], $p(y_i/x_i) = \frac{y_i}{f(x_i)} e^{-\frac{y_i^2}{2f(x_i)}}$. Assuming that $x_i$ are accurately measured, the likelihood function is

$$l(V,U) = \sum_i \log\left[\frac{y_i}{f(x_i)}\right] - \frac{y_i^2}{2f(x_i)} \tag{2}$$

In this paper $U$ is modeled as a Markovian random field with a Gibbs distribution,

$$P(U) = \frac{1}{Z} e^{-\frac{\alpha}{N'_v} \sum_{p \in G} \sum_{g \in \delta'_p} (u_p - u_g)^2} \quad (3)$$

where $Z$ is a partition function, $G$ is the set of all index of $U$ and $\delta'_p$ is the set of all $N'_v$ backwards neighbors of $u_p$.

The goal of 3D reconstruction is to estimate $U$, using the available observations $V$.

Note that there is no direct relation (one to one) between the coefficients to estimate, $u_i$ and the observations $v_i = (y_i, x_i)$. In this situation the prior distribution plays an important role, making it possible to estimate coefficients that are not directly observed and must be estimated from its neighbors.

Adopting a MAP estimation procedure, $U$ is the solution of the optimization problem,

$$\hat{U} = arg \max_U E(U, V) \quad (4)$$

where,

$$E(U, V) = -l(U, V) - \log(p(U)) \quad (5)$$

The solution of (4) is obtained by using numerical methods. Since $U$ has thousands of coefficients, the optimization procedure is computationally expensive. To solve (4) the ICM [6] algorithm is used. This algorithm minimize the energy function with respect to one coefficient at a time keeping the other constant. This algorithm transforms the n-dimensional optimization problem in a set of 1-dimensional optimization problems (see [4] for details).

The solution of (4) using the ICM method leads to a set of non-linear equations where all the ultrasound images are processed, in each iteration, because it is not possible to compute sufficient statistics. Therefore, the reconstruction algorithm is computationally demanding and slow.

To speed up the reconstruction process a simplification was proposed in [3] by deriving a linear set of equations using sufficient statistics. With this simplification it was possible to reduce the processing time by up to one order of magnitude. In the next section we briefly present this method which is the starting point for the algorithm described in this paper.

## 3. LINEAR MAP RECONSTRUCTION

Consider the log likelihood, $l$ as a function of a single coefficient $u_p$ as in the ICM method and let us expand $l(u_p)$ in Taylor series in the vicinity of the maximum likelihood estimate, $u^{ML}$.

Discarding the terms of order higher then two

$$l(u_p) \simeq l(u_p^{ML}) + l'(u_p^{ML})(u_p - u_p^{ML}) + \frac{1}{2} l''(u_p^{ML})(u_p - u_p^{ML})^2 \quad (6)$$

To solve (4) with respect to $u_p$ the following stationary condition should be met

$$\frac{\partial E(U, V)}{\partial u_p} = 0 \quad (7)$$

where the log likelihood function $l(u_p)$ used is replaced by (6).

The first derivative of (6) with respect to $u_p$ is

$$\frac{\partial l(U)}{\partial u_p} = l''(u_p^{ML})(u_p - u_p^{ML}) \quad (8)$$

because the derivatives of the first and second terms of the right side of (6) vanish. The first term is constant and the second is null by definition, since $u_p^{ML}$ is the log likelihood estimate.

Under the above conditions, and using the fixed point method, the equation (7) is solved by the recursive equation

$$\hat{u_p} = \frac{1}{4\alpha} l''(u_p^{ML})(u_p - u_p^{ML}) + \bar{u}_p \quad (9)$$

This equation can be approximated [3] by

$$\hat{u}_p = (1 - k_p) u_p^{ML} + k_p \bar{u}_p \quad (10)$$

where $\bar{u}_p = \frac{1}{N_v} \sum_{g \in \delta_p} u_g$, $k_p = \frac{1}{1+\tau_p}$ and $\tau_p = \frac{1}{4\alpha} \frac{\sum_i \phi_p(x_i)}{(u_p^{ML})^2}$ with $\delta_p$ the neighborhood of $u_p$ and $N_v$ the number of elements of $\delta_p$ (see [3] for details).

Equation (9) computes the MAP volume estimate by the solution of a set of linear equations whose coefficients are computed at once for all at the first iteration. Furthermore, recursion (10) converges faster than the ICM algorithm applied to (5) being, at the same time, more stable. This approximation speeds up the estimation process by one order of magnitude, without degradation of the reconstruction results.

The next section provides a new algorithm which allows to reduce the computational time even more.

## 4. IIR FILTER

Equation (10) defines a IIR filter. This filter is not wedge supported [7]. Each output depends on past and future outputs since it depends on $\bar{u}_p$. Therefore, it is not possible to recursively compute the output. To overcome this difficulty we consider a set of eight wedge supported filters (see Fig.4), which can be recursively computed. The output of the original filter is approximated by averaging the output of all these eight filters. Each of these filter starts from a different corner of the volume using the previous computed nodes, i.e.,

$$(u_w)_p = v_p + (\bar{u_w})_p \quad (11)$$

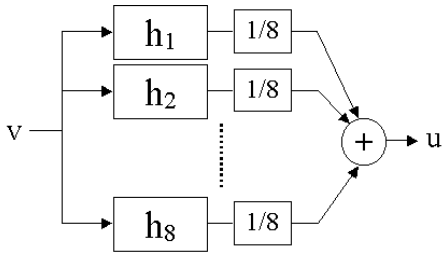


**Fig. 1**. Bank of eight filters.

| Algorithm | L | S/N(dB) | Time(s) |
|---|---|---|---|
| MAP | -1.06e7 | 23.54 | 502.24 |
| Taylor | -1.06e7 | 23.04 | 95.67 |
| IIR | -2.20e7 | 22.54 | 20.26 |

**Table 1**. Reconstruction results with synthetic data (128 images).

where $w = 1, 2, ..., 8$, $v_p = (1 - k_p)u_p^{ML}$ and $p = (i, j, k)$.

For instance, the filter $h_1$, is computed by starting at the node $(u_1)_{(0,0,0)}$ and a generic coefficient is computed using

$$(u_1)_{(i,j,k)} = v_{(i,j,k)} + (\bar{u_1})_p \tag{12}$$

where $(\bar{u_1})_{(i,j,k)} = ((u_1)_{(i-1,j,k)} + (u_1)_{(i,j-1,k)} + (u_1)_{(i,j,k-1)})/3$. In the case of the filter $h_2$ the starting node is $(u_2)_{(N-1,0,0)}$ and to estimate a generic node the averaging nodes are $(u_2)_{(i+1,j,k)}$, $(u_2)_{(i,j-1,k)}$ and $(u_2)_{(i,j,k-1)}$.

With this approach we can solve the huge set of equations (10) in a non iterative way, with significant computational gains.

## 5. EXPERIMENTAL RESULTS

Experimental tests were carried out to assess the performance of the proposed method using synthetic and real data. Three reconstruction methods were considered: the NLMAP method (see section 2), the LMAP method (see section 3) and the IIRMAP method (see section 4). To compare the results obtained by the three methods, processing times, profiles and surfaces are computed. In the case of synthetic data it was computed the signal to noise ratio since the original volume is known.

Let us briefly describe the experiment with synthetic data. A set of $128$ images with $128 \times 128$ pixels were processed. These images correspond to parallel cross-sections extracted from a volume containing a sphere. This volume is binary, i.e., the background has a constant value and the sphere has another constant value. The images were corrupted with Rayleigh noise. Table 1 summarizes the results of the three reconstructions. The proposed method is $25$ times faster than the NLMAP algorithm in this example, exhibiting a slight degradation in SNR. Fig.2 shows cross-sections extracted from the original volume and from the reconstructed volumes. All methods produce comparable results. The results of the IIR filter is slightly more noisier. Fig.3 shows the same intensity profiles extracted from Fig.2. The proposed algorithm was used in the reconstruction of human organs. The next example, considers a set of $62$ images with $176 \times 176$ pixels corresponding to cross-sections of a gall bladder. Fig.5.a) shows an ultrasound image and Figs.5b-d) shows the corresponding cross-sections obtained from the reconstructed volumes using the b)NLMAP, c)LMAP and d)IIRMAP methods. The main diagonal profiles of these cross-sections are shown in Fig.3 and the surfaces corresponding to the sphere boundaries obtained from the estimated volumes are shown in Fig.4.

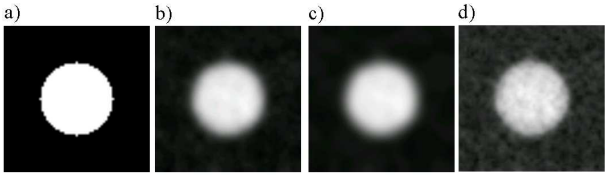


**Fig. 2**. Cross sections of the a)original volume and from the reconstructed volumes obtained using the b)NLMAP, c)LMAP and d)IIRMAP methods with synthetic data.

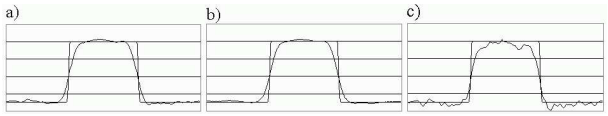


**Fig. 3**. Profiles of the reconstructed volumes obtained using the a)NLMAP, b)LMAP and c)IIRMAP methods with synthetic data.

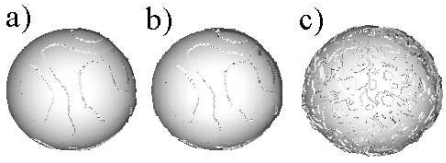


**Fig. 4**. Surface extracted from the estimated volumes using the a) NLMAP, b)LMAP and c)IIRMAP methods with synthetic data.

To compare the data extracted from the reconstructed volumes with the ultrasound image the following transform was used: $g = \sqrt{\frac{\pi f}{2}}$. This is the expression of the expected value of a Rayleigh distribution with parameter $f$. These images and profiles show that the three reconstructions are similar. The surfaces extracted from the three estimated volumes are shown in Fig.7. There is no significant

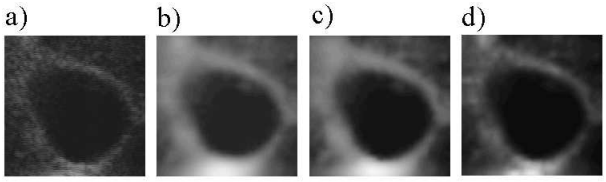


**Fig. 5**. Cross sections of the a)original volume and from the reconstructed volumes obtained using the b)NLMAP, c)LMAP and d)IIRMAP methods with real data.

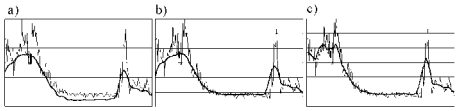


**Fig. 6**. Profiles of the reconstructed volumes obtained using the a)NLMAP, b)LMAP and c)IIRMAP methods with real data.

degradation of the reconstruction results obtained by using the fast IIRMAP algorithm.

Table 2 shows that the IIRMAP method is faster about $25$ times than the NLMAP and $4.5$ times faster than the LMAP method. Besides the benefits in processing times, the IIRMAP method it is also much more stable. In fact, it has no convergence problems. On the contrary, the NLMAP algorithm presents a narrow convergence range. For small values of the regularization parameter, $\alpha$, the algorithm diverges. In that case, several measures can be taken to enforce the convergence. One of them consists of adding an offset to the observed data to avoid small values that are responsible for the divergence. A second approach is to decrease the $\alpha$ parameter during the optimization process starting with a strong regularization. None of these difficulties is present in the case of IIRMAP filter.

## 6. CONCLUSIONS

In this paper we present a reconstruction algorithm for freehand 3D ultrasound. The observed data is formed by a set of ultrasound images complemented with the information of position and orientation of each image in the 3D space. The algorithm is design in a Bayesian framework but implemented by a set of recursive filters. We derive the expressions of these filters with data dependent coefficients

| Algorithm | L | Time(s) |
|---|---|---|
| MAP | -7.29e06 | 469.50 |
| Taylor | -7.29e06 | 85.10 |
| IIR | -3.33e07 | 18.77 |

**Table 2**. Reconstruction results with real data ($62$ images).

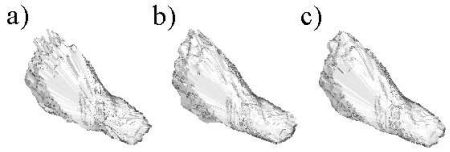


**Fig. 7**. Surfaces extracted from the reconstructed volumes using the a)NLMAP, b)LMAP and c)IIRMAP methods with real data.

from the expressions of the MAP estimation. The output of the filter is similar to the MAP solution but the algorithm is less time consuming. The goal is to obtain the benefits of the Bayesian methodology with the computational efficiency of the recursive processing. To test the algorithm, two examples using synthetic and real data were presented. The proposed algorithm manages to reduce the computation time by a factor of $25$ achieving comparable reconstruction results. A slight degradation of quality was observed in the case of synthetic data but no degradation was observed with real data. Furthermore, the proposed method is more robust than the other iterative methods presented.

## 7. REFERENCES

[1] R. Rohling et al. Radial basis function interpolation for 3D freehand ultrasound. In Proceedings of the 16th International Conference on Information Processing in Medical Imaging, pages 478-483, Visegrd, Hungary, June 1999 (LNCS 1613, Springer).

[2] T.A.Gooley et al., Evaluation of Statistical Methods of Image Reconstruction Through ROC Analysis, IEEE TMI, vol.11, no.2, June 1992.

[3] J.Sanches and J.S. Marques, A Fast MAP Algorithm for 3D Ultrasound, Proceedings 3th EMMCVPR2001, pp.63-74, France, September 2001.

[4] J. Sanches, J. Marques, A Rayleigh reconstruction/interpolation algorithm for 3D ultrasound, Pattern Recognition Letters, 21, pp.917-926, 2000.

[5] C. Burckhardt, Speckle in Ultrasound B-Mode Scans, IEEE Trans. on Sonics and Ultras., vol. SU-25, no.1, pp.1-6, Jan. 1978.

[6] J. Besag, On the Statistical Analysis of Dirty Pictures, J. R. Statist. Soc. B, vol.48, no. 3, pp. 259-302, 1986.

[7] Jae. S. Lim, Two-Dimensional Signal and Image Processing, PTR Prentice Hall, Englewood Cliffs, New Jersey.